Eur. Phys. J. D **33**, 49–57 (2005)
DOI: 10.1140/epjd/e2005-00035-7

THE EUROPEAN PHYSICAL JOURNAL D

Dynamics of H_9^+ in intense laser pulses

M. Ma[1], P.-G. Reinhard[2], and E. Suraud[1,a]

[1] Laboratoire de Physique Théorique, Université Paul Sabatier, 118 route de Narbonne, 31062 Toulouse Cedex, France
[2] Institut für Theoretische Physik, Universität Erlangen, Staudtstrasse 7, 91058 Erlangen, Germany

Received 21 June 2004 / Received in final form 8 February 2005
Published online 11 April 2005 –

Abstract. We discuss the response of the H_9^+ cluster to an excitation by an intense laser beam. Calculations are done within the framework of TDLDA-MD, an approach which has proven to provide a robust tool for investigations in metal cluster dynamics. We first discuss static and low energy properties of H_9^+ and make comparisons with other existing ab initio results. We then explore the various excitation/deexcitation scenarios as a function of the laser parameters.

PACS. 36.40.Wa Charged clusters – 36.40.Qv Stability and fragmentation of clusters – 36.40.Cg Electronic and magnetic properties of clusters

1 Introduction

The recent developments in laser technology have opened up several directions of research, for example in the analysis of the dynamical scenarios following an excitation of molecules and clusters with fs laser pulses. Such a powerful tool is extremely versatile to trigger and to analyze a world of dynamical processes. These processes cover a bunch of various dynamical situations, ranging from the "simple" optical response [1] to multi-photon ionization [2], and further on to the various scenarios of Coulomb explosion of clusters [3,4], for a broad survey see [5]. An appropriate theoretical description of such involved processes requires a fully-fledged coupled ionic and electronic dynamics. Indeed the violent excitations by fs lasers quickly drive the system beyond the Born-Oppenheimer surface. From the electronic point of view, time dependent Density Functional Theory at the level of the time-dependent local-density approximation (TDLDA) [6] offers a well tested and robust tool. One usually treats the ions by classical molecular dynamics (MD). This altogether provides a coupled TDLDA-MD, for a review see [7].

A few studies of dynamical scenarios using TDLDA-MD are already available, in particular in simple metal clusters [8,9]. There is a world of other materials to be attacked with TDLDA-MD. One particularly interesting case are hydrogen clusters. Indeed, hydrogen is a generic material whose metallic or non-metallic behavior has raised much attention recently [10]. Furthermore Coulomb explosion of hydrogen clusters seems to be an extremely interesting process [3], for example for possible table top fusion experiments, when the heavy isotope of hydrogen, deuterium, is used. It should also be noted that switching from simple metals to hydrogen clusters is a challenging test for the model. Indeed, the hydrogen bond is very different from the strongly delocalized simple metallic bond. It is hence interesting to test the capability of LDA in such a situation. Many works have been done on hydrogen clusters. In this work we present some results on H_9^+ irradiated by a laser. This cluster possesses a well studied ionic configuration [11–14] exhibiting well structured coupling pattern with light. It is hence ideal for testing purposes.

2 Framework

Many refined approaches may be (and are) used for cluster structure calculations. But dynamical applications are better done with a robust and efficient scheme. A standard tool in that respect is meanwhile time-dependent density functional theory employing the instantaneous local density, i.e. the time-dependent local-density approximation TDLDA [15]). We work here with pure LDA (for spin saturated systems) and employ the exchange-correlation functional of [16]. Details on this general treatment of electrons in particular in the case of far off equilibrium situations can be found in [5,7].

The interaction between ions and electrons is described by means of a local pseudo-potential which consists out of a sum of two error functions

$$V_{\rm psp} = -\frac{Ze^2}{r}\left\{c_1 \mathrm{erf}\left(\frac{r}{\sqrt{2}\sigma_1}\right) + c_2 \mathrm{erf}\left(\frac{r}{\sqrt{2}\sigma_2}\right)\right\} \quad (1)$$

with $c_1 = 1.809$, $c_2 = -0.8094$, $\sigma_1[\mathrm{a}_0] = 0.2548$ and $\sigma_2[\mathrm{a}_0] = 0.3822$. We employ here a pseudopotential

[a] e-mail: suraud@irsamc.ups-tlse.fr

instead of the well-known correct potential e^2/r for numerical purposes. Indeed the pure Coulomb potential does not comply well with a description of the wavefunctions on a spatial grid as we use. The pseudopotential allows to adjust the spectrum correctly by carefully counterweighting the smoothing at smallest r. The used pseudopotential has rather large folding radii, because the smallest grid spacing has to be proportional to the smaller of the two widths ($\Delta = \sigma_1\sqrt{2\log 2}$). We can thus work here with a grid spacing of $\Delta = 0.3\,\mathrm{a_0}$ which yields an extremely efficient numerical handling, in particular for "large" systems.

Ions are treated as classical particles and propagated under their mutual (point-like) Coulomb interactions together with the electron-ion forces as derived from the pseudo potential. The laser field, acting both on electrons and ions, reads $V_{\mathrm{las}} = E_0\hat{d}f_{\mathrm{las}}(t)\cos(\omega t)$ ($\hat{d}$ being the local dipole operator and $E_0 \propto \sqrt{I}$, I being the intensity). The pulse profile is chosen as a cosine^2 in time and the pulse duration can be characterized by the FWHM of the profile function $f_{\mathrm{las}}(t)$. The TDLDA equations are then solved numerically on a grid in 3D coordinate space (cubic box size of 72^3). The ground state wavefunctions are determined by an accelerated gradient step [17]. The time-dependent Kohn-Sham equation for electrons is solved with the time-splitting technique [18] and a Verlet algorithm [19] is used for the simultaneous ionic propagation. We employ absorbing boundary conditions to treat ionization correctly [20]. More details of this treatment can be found in [7]. Note that this coupled ionic and electronic dynamics goes beyond the usual Born-Oppenheimer MD. This is needed to cope with the violent off-equilibrium dynamics as induced by strong laser pulses. The capability of this technique to deal with small hydrogen clusters was furthermore demonstrated earlier [21].

In the present work we are interested on the following observables: ionic configurations, ionic moments, electron density or moments thereof, ionization, and excitation spectra. The ionic positions and electron density are part of the calculations and trivially accessible. Ionization is computed from the norm of the electron density on the grid. Note that this norm decreases and this decrease expresses just the electrons absorbed at the bounds, i.e. the finally emitted electrons. The spectral distribution of dipole strength is computed by exerting an instantaneous dipole boost, then taking a protocol of the electronic dipole moment in time and finally Fourier transforming into the frequency domain [7,22,23].

3 Basic features

3.1 Ionic structure

The first step is to find the ground state configuration of the system, here of the H_9^+ cluster. As a practical method, we use full TDLDA-MD in a "cooling" version. An initial "guess" configuration which is not fully equilibrated exerts forces on the ions which, in turn, start to move. Once in a while, we remove the kinetic energy from the ions. This then cools down the cluster systematically until the energetic minimum configuration is found. This simple and straightforward technique terminates in a local minimum. A broad variation of initial conditions is required to specify the global minimum. The situation for H_9^+ is greatly simplified by the fact, that there exist already several quantum chemical investigations of hydrogen structures, see e.g. [11–14]. These calculations show that H_{2n+3}^+ clusters exhibit structures with a central H_3^+ core surrounded by regularly distributed, more loosely bound, H_2 dimers. We start from such a structure which will most probably yield also the ground state configuration for our treatment. We have additionally tried several much different starting points, including metallic-like structures, and always end up in the same type of configuration (up to details), namely a H_3^+ central piece surrounded by H_2 dimers. Actually, we cool down the system to about 50 K temperature which is sufficient for the present studies. The result of our structure optimization is shown in Figure 1. The dimer bond in hydrogen is so strong that the system hesitates to break it. The same holds for the positively charged trimer. As a consequence, H_9^+ is formed as a molecule of dimers and a central trimer with a weak binding between them. Complementing information on the bond lengths is provided in Table 1. It corroborates the visual impression. Actually, the bond length between the constituents is almost twice as large as those inside a building block. The present LDA calculations reproduce the quantum chemical calculation of [12] within 10%. That corroborates our earlier calculations on simpler Hydrogen clusters (namely H_2 and H_3^+), the results of which matching again other calculations and experimental data (bond length, Ionization potential) [21]. Conversely, the 10% difference may be attributed to the use of mere LDA. The strong spatial variations in hydrogen systems would require gradient terms added to LDA [24] and/or self-interaction correction [25]. However, the present precision suffices for our intended explorations on cluster dynamics far off equilibrium, which aims more at working out trends.

Table 1. The bond length for the substructures of the H_9^+ cluster of Figure 1, in units of $\mathrm{a_0}$. The last line provides the distance between center of masses of dimers to trimer. The second column shows results from our calculations, the third line those of [12].

	present	from [12]
dimers	1.57	1.41
trimer	1.92	1.68
dimers/trimer	3.00	3.12

3.2 Optical absorption spectra

In the optical domain, a laser field dominantly couples to the cluster by the dipole operator. The doorway to dynamics is then the spectrum of dipole oscillations of the system. This has always to be studied first before any

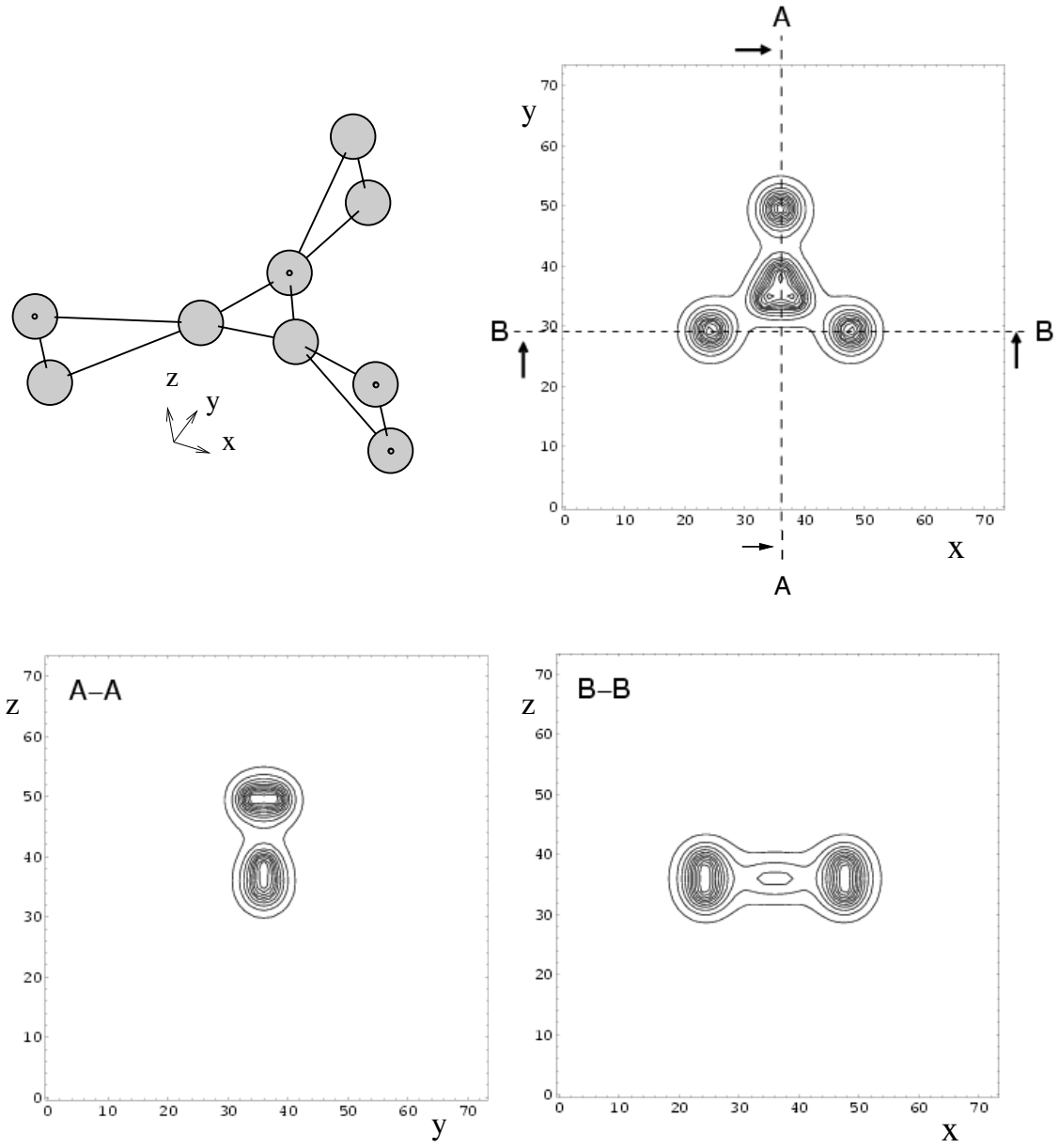

Fig. 1. Ionic structure (upper left panel) and electronic density of H_9^+. The density is shown in three cuts: upper right = in the x-y-plane, lower left = in the y-z-plane along line A–A indicated in the upper right panel, lower right = along x-z-plane along line B–B indicated in the upper right panel (i.e. a cut through a dimer). The x-, y-, and z-directions are indicated in the upper left panel.

fancier dynamical application. Figure 2 shows the dipole strength for H_9^+ separately for each direction (note that oscillations in x are equivalent to those in y for symmetry reasons). The strong electronic binding in the dimer and trimer leads to rather high excitation energy in the far UV range, as is typically to be expected for hydrogen systems. The mode in z-direction shows two pronounced peaks which can be associated, although significantly shifted, with modes of the dimer or trimer constituents. The peak at 12.7 eV belongs predominantly to the dimers and represents a combined action of the three dimer clouds oscillating along their long axis, perpendicular to the symmetry plane of the molecule. This mode is found at 18 eV in a separate dimer. It emerges here at the much lower frequency of 12.7 eV due to collective coupling. The peak in the z-spectrum at 15.6 eV belongs to a vibration in the trimer. It is related to a mode at 20.8 eV in the free trimer oscillating orthogonal to the trimer plane. These two modes are well isolated in energy and they allow to excite the system in two geometrically very different manners. We will use them later on as a practical doorway for dedicated excitations with strong lasers. The spectrum in x-y-direction is a bit more fragmented. That happens because the modes mix more strongly.

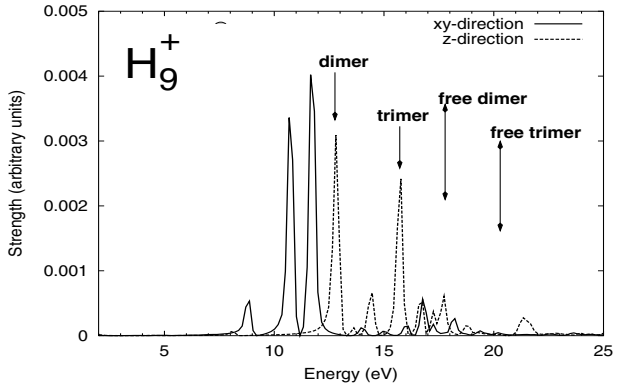

Fig. 2. Spectral distribution of dipole strength in the $x(\equiv y)$-direction (solid lines) and z-direction (dotted). The peaks associated with predominant excitation of the dimer-part and trimer-part of H_9^+ are indicated. The frequencies of the corresponding excitations in free dimers and trimer cation are indicated by vertical lines with double arrow.

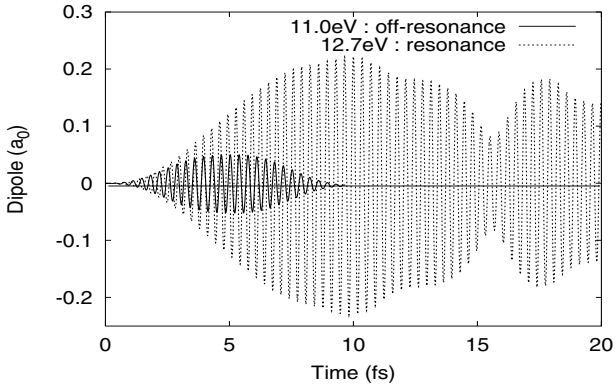

Fig. 3. Time evolution of dipole moment for two different laser excitations, one with $\hbar\omega_{\rm las} = 11.0$ eV off resonance and a resonant one at $\hbar\omega_{\rm las} = 12.7$ eV. Both pulses have polarization in z-direction, intensity $I = 1.8 \times 10^{12}$ W/cm^2, and FWHM 5 fs.

4 Dynamics driven by laser fields

As was described in Section 2, the laser is coupled to the cluster as a time-dependent classical field interacting simply via the dipole operator. Less simple is the choice of the test case in the enormous variety of conceivable laser parameters. We characterize the pulse by frequency, width (extension in time), and intensity. And all these parameters have their specific influence [26]. The frequency is the most important parameter in all regimes because it determines the strength of the laser-cluster coupling. The intensity determines the dynamical regime. Very low intensities apply to the regime of (linear) optical response. Moderate intensities allow for non-linear effects as higher harmonic generation and dedicated dynamical switching. Very large intensities lead into the regime of the nanoplasma and brute-force Coulomb explosion [3]. We will deal here with moderately large intensities. The width of the pulse determines the spectral resolution and the interplay with ionic motion. We use here pulse lengths with FWHM of 5–10 fs which are just long enough for sufficient resolution. They, nonetheless, interfere slightly with the ionic motion which is particularly fast for the protons in hydrogen. The following investigation concentrate on variations of frequency and intensity.

4.1 Resonance: on versus off

It makes a principle difference whether the laser frequency hits a resonance frequency of the system or whether it is off resonance. Figure 3 shows an example of dipole response in an off-resonance ($\hbar\omega_{\rm las} = 11.0$ eV) and a resonance case ($\hbar\omega_{\rm las} = 12.7$ eV). In both cases the laser intensity is $I = 1.8 \times 10^{12}$ W/cm^2, pulse FWHM of 5 fs, and polarization along z-direction (perpendicular to the H_9^+-"plane"). The intensity is larger than one typically takes to explore linear response, but still sufficiently moderate to leave the system basically intact. In an off-resonance case, the dipole response is expected to follow exactly the excitation field and to dissappear when the excitation is switched off [27]. That is indeed the case in Figure 3 where we can recognize the shape of the 10 fs (total duration) laser pulse. In the case of a resonant excitation, the system reacts much more heftily which is related to resonant field amplification [28,29]. The dipole amplitude keeps growing as long as the laser is irradiating the cluster. And strong oscillations keep going long after the laser has been switched off. The beating seen in the late dipole response is due to the slight fragmentation of the spectrum, see Figure 2, and a corresponding slight mix of eigenmodes in the actual excitation (mind that 10 fs pulse width yield a spectral resolution of about 0.5 eV). In fact, the post-laser dynamics in the off-resonant case is mainly driven by ionic motion whereas electronic dynamics dominates in the resonant case. In other words, in the off-resonance case, the electrons follow the ions, whereas in the resonant case, the ions follows the electrons. This mechanism will show up also later on in this work.

It should finally be noted that the excitation strength, i.e. the dipole amplitude, has consequences for direct electron emission, as was already discussed in [27] in the case of small metal clusters. A large dipole amplitude is related to strong emission while small amplitudes produce only weak emission. We shall see later on the consequences of these emission pattern on the evolution of the system.

4.2 Two different resonances

In the previous Section 4.1, we have discussed the difference between resonant and off-resonant excitation. The spectra in Figure 2 display two strong resonances for excitation in z-direction. It is worth checking the influence of the resonance through which the excitation goes on the subsequent dynamics. Let us briefly recall that the system is composed of a trimer cation at the center and three dimers attached to it. The two strong peaks for z-modes correspond to dimer excitation for 12.7 eV, and to trimer

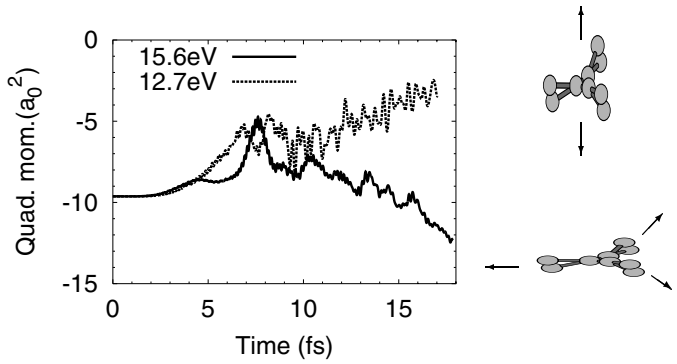

Fig. 4. Time evolution of electronic quadrupole moment along z-axis, Q_{20}, after excitation by two laser pulses with intensity 1.8×10^{13} Wcm^2, pulse FWHM of 5 fs, and two different frequencies as indicated. The different frequencies couple to different modes as indicated in the two schematic views at the right side of the plot.

excitation at 15.6 eV. The dynamics should be different depending on which mode is excited by the laser. To test that, we chose a pulse with intensity of 1.8×10^{13} Wcm^2 and FWHM of 5 fs. This yields about the same dipole amplitude for both photon energies (12.7 and 15.6 eV) and subsequent electron emission (10.5% namely about 1 electron). And yet, the distribution of excitation energy within the cluster differs. At laser frequency $\hbar\omega_{\rm las} = 12.7$ eV, the energy will be absorbed by the dimers and we expect that this leads to their dissociation in the z-direction. At $\hbar\omega_{\rm las} = 15.6$ eV, it is the trimer which is predominantly excited and we expect strong breathing of the trimer around its center of mass which will shake-off the dimers.

To analyze the different dynamical evolutions, we calculate the quadrupole deformation of the system along z-direction, i.e.

$$Q_{20} = 2\langle z^2\rangle - \langle x^2\rangle - \langle y^2\rangle \qquad (2)$$

where the brackets mean quantum mechanical expectation values for the electrons or classical averages for the ions. The value $Q_{20} = 0$ characterizes a spherical shape, $Q_{20} < 0$ indicates oblate and $Q_{20} > 0$ prolate shapes, as measured with respect to the "molecule x-y-plane". In its ground state H_9^+ is strongly oblate with its almost "planar" structure. Figure 4 shows the time-evolution of the quadrupole moment after excitation through the two different resonances (at 12.7 eV and 15.6 eV respectively). The differences between the two cases are obvious. Both excitations yield first a move towards less oblate deformation. This is related to the fact that in the early stages of the response the system undergoes some radial expansion. Later on, the upper resonance drives back to even more oblate shapes (more negative value of Q_{20}). That indicates the three dimers flying apart along the symmetry plane of the original cluster. The excitation through the lower resonance (dimer modes), however, shows steady increase of Q_{20} to less and less oblate configurations. This complies with the picture that the dimers are dissociating into hydrogen atoms and each atom flies apart orthogonal to the symmetry plane. Altogether, Figure 4 nicely demonstrates that the dynamical evolution can be switched in one direction or another by tuning the laser frequency.

4.3 A more detailed look at coupled dynamics

In this section, we will investigate the detailed time evolution for four observables, electron emission, ionic coordinates, radii, and quadrupole moments. The latter two observables are shown for ions as well as for electrons. Two very different laser frequencies are considered, the first one is in the visible range at 2.33 eV far below any eigenfrequency of the cluster, and the second one at 15.6 eV which is in resonance with the trimer mode in z-direction (see Sect. 3.2). For both frequencies, we consider a low intensity with low emission around one electron and a large intensity causing strong electron emission (around six electrons). The laser polarization was chosen along the diagonal in x+y+z-direction to mimic the arbitrariness of polarization axes if the laser shines on a thermal ensemble of free clusters. The pulse width (FWHM) was in all cases 10 fs.

4.3.1 Resonant — low emission

Figure 5 shows details for the excitation in resonance with the state at 15.6 eV (where the trimer is preferably shaken). Here we consider again a moderate intensity of $I = 1.8\times10^{13}$ W/cm^2 which stays in a regime where about one electron is emitted in the course of the laser pulse. The electronic radius shows a large increase at around 10 fs which is the time at which the laser pulse has maximum amplitude. The increase reflects the strong electronic dipole response (see e.g. Fig. 3) which blows up the electron cloud as a whole. It is also at this time that electron emission is strongest. This can be seen from the uppermost panel. The strongest slope resides around 12.5 fs which is the peak time of the laser pulse plus some additional time taken by the electrons to leave the box. Coming back to the radii, we also see the ionic radius reacting with a steady increase starting at about 15 fs. The reaction is a bit delayed because ions are more inert than electrons. And yet, this delay of a few fs is unusually short as compared to ionic motion in clusters with heavier elements [30]. The detailed z-coordinates of the ions are shown in the second panel. The initial configuration is mapped here as the three ions of the trimer reside at $z \sim 0$ and the six ions of the dimers at ±0.8 a$_0$. The trimer ions remain more or less in the $z = 0$-plane while the dimer ions start to oscillate strongly but also seem to remain bound in z-direction. In fact, the main motion is an expansion inside the x-y-plane. This can be deduced from the quadrupole moment shown in the lowest panel of the figure. One can also compare ionic and electronic Q_{20} in that plot. The electrons show a stronger direct response to the laser field around 10 fs. But the perturbation is weak enough to leave only little excitation (i.e. electrons staying still close to the ions). Thus they follow the global ionic

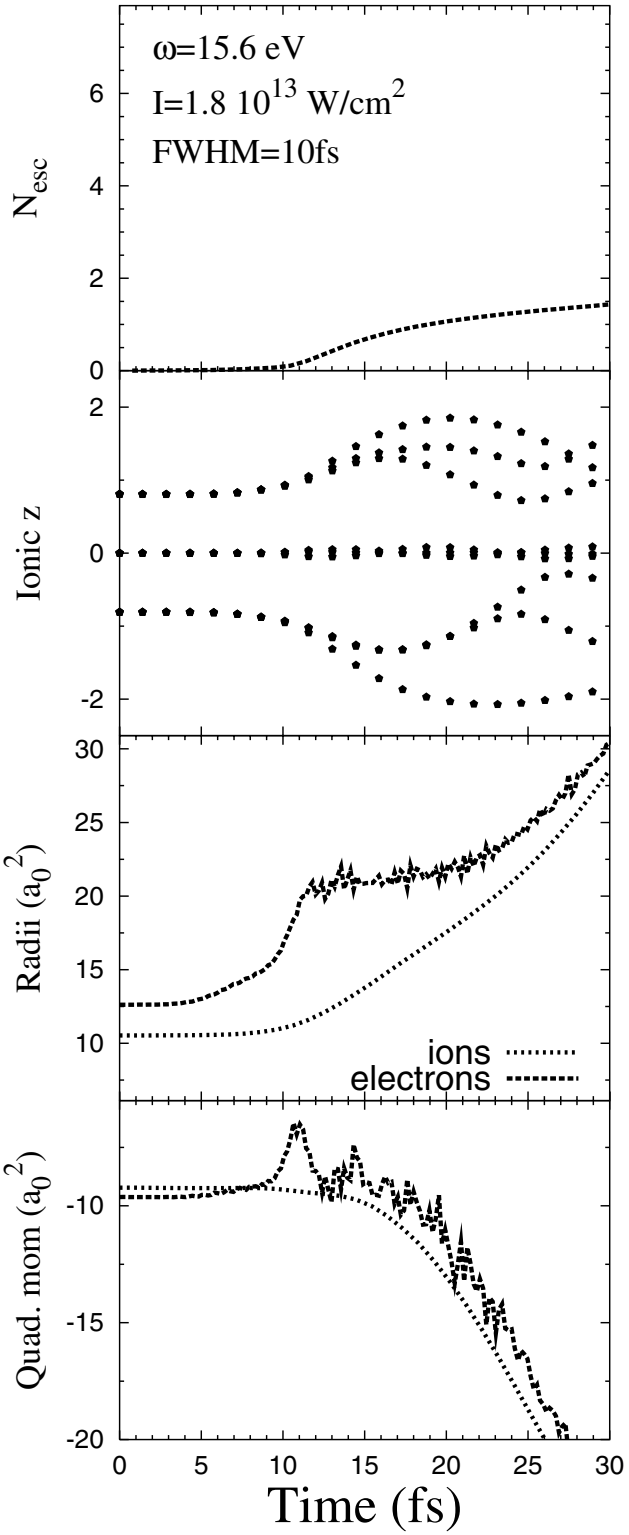

Fig. 5. Time evolution as triggered by laser excitations for various observables: uppermost = number of emitted electrons, second from above = ionic z coordinates, third from above = r.m.s. radii of electrons (dashed) and ions (dotted), lowest = quadrupole momentum Q_{20} as defined in equation (2) for electrons (dashed) and ions (dotted). The laser was polarized along the x+y+z-diagonal. The other laser parameters are given in the uppermost panel.

motion in the further course of the dynamical evolution. And this evolution is clearly characterized by a dissociation into dimers and trimer taking place essentially along the x-y-plane.

4.3.2 Resonant — high emission

Figure 6 shows results again from excitation at 15.6 eV but with larger intensity and subsequently much enhanced electron emission. Five to six out of the eight electrons are removed in a comparatively short time. At that charge state, the cluster is grossly Coulomb unstable. And correspondingly, all ionic observables show clearly the pattern of a straight Coulomb explosion. There are nevertheless two interesting differences as compared to the previous case at moderate intensity. First, the electronic moments deviate from the ionic ones in the late stages, and second, the ionic expansion goes through prolate shapes rather than oblate ones. The first effect becomes understandable when realizing that only charge two to three is left for the electrons. Most of the ions are leaving the system nearly naked which decouples electronic and ionic densities. The second effect is related to the particular spatial structure of H_9^+. The ions in dimers repel each other strongly once they have lost their electrons. This drives them to separate quickly in $\pm z$-direction as seen in the second panel (from top). The trend is faster than the Coulomb expansion in the x-y-plane. And this, in turn, yields a quickly growing prolate quadrupole moment.

4.3.3 Off resonant — low emission

Figure 7 shows the result from excitation with a comparatively low frequency of 2.3 eV. The intensity looks large as compared to the previous cases. But its effect is only moderate because the case is far off resonance. Only about one electron is emitted in the course of the laser pulse which is comparable with the resonant low emission case, discussed in Section 4.3.1. The frequency is far below all eigenmodes of the system such that one may speak of an adiabatic excitation. Let us first look at the radii. The electronic radii show a bump around 10 fs which is the time where the laser pulse has maximum amplitude. The bump reflects the strong electronic dipole response (see e.g. Fig. 3). It is the time at which electron emission is strongest. This can be seen from the uppermost panel. The strongest slope resides around 12.5 fs which is the peak time of the laser pulse plus some additional time taken by the electrons to leave the box. Coming back to the radii, we see ionic motion starting with a small bump around 15 fs. This is the ionic response to the electronic breathing and changed charge state. It comes with a delay because ions are more inert than electrons. But again, this delay of a few fs is unusually small due to the comparatively low proton mass. After a first oscillation, the ionic structure seems to expand and the electron cloud is following willingly this ionic trend, similar as it was observed in the resonant low emission case in Section 4.3.1 but differently from the violent explosion.

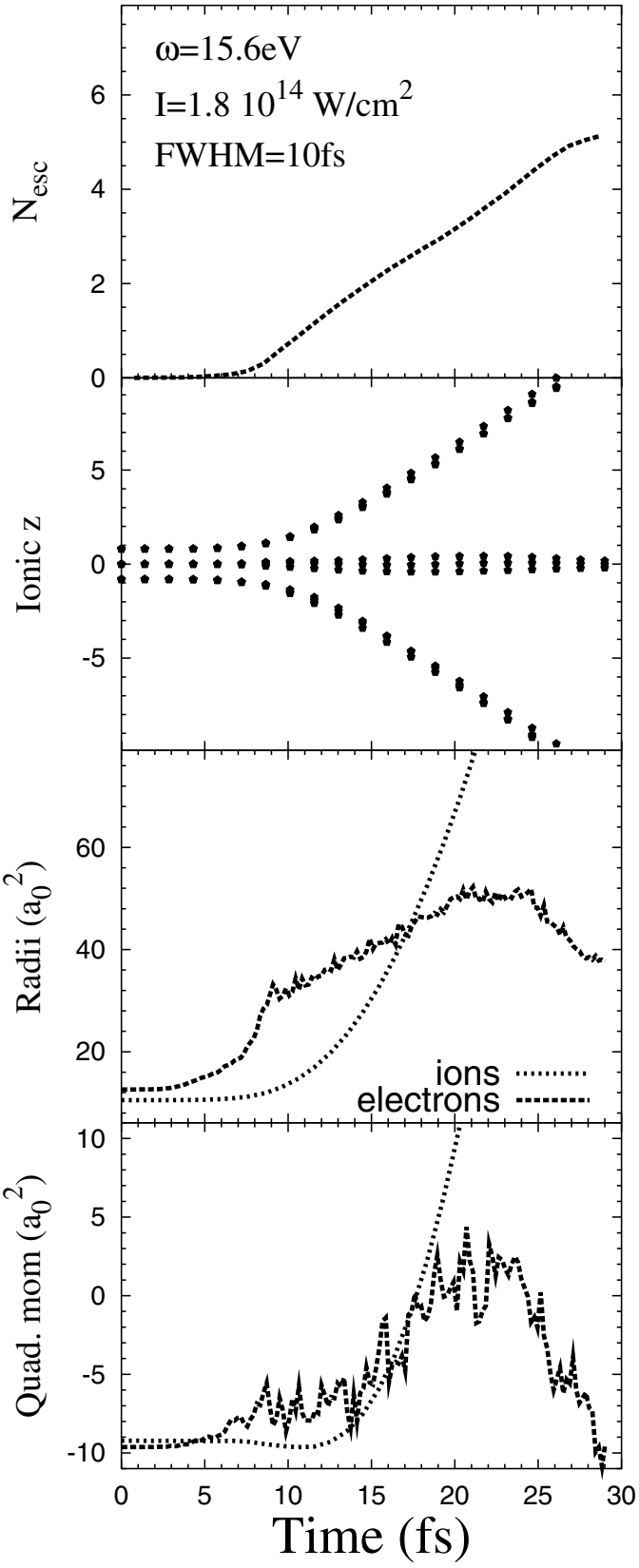

Fig. 6. As Figure 5, but with higher intensity.

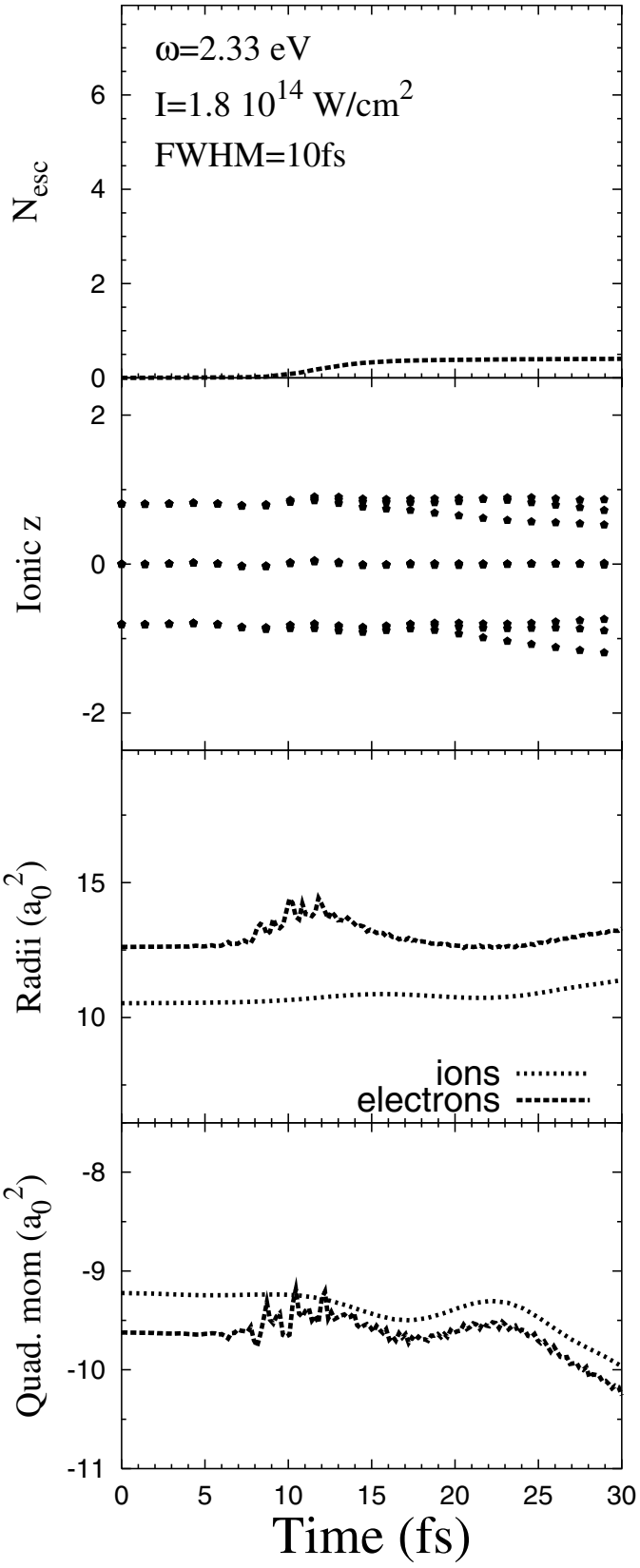

Fig. 7. As Figure 5, but now with frequency of 2.3 eV, far below any resonant state. The intensity is related to a low emission regime.

The detailed z-coordinates of the ions are shown in the second panel of Figure 7. Most interesting is the late phase in the plot. The trimer ions remain in their plane while the dimer ions start to move. One can read off that the bond lengths do not change so much and the dimers as a whole drift in slightly different directions. The main expansion takes place in the x-y-plane as can be seen again from the quadrupole moment (shown in the lowest panel of figure) which develops towards increasingly oblate shapes. Altogether, the global pattern for this case far below resonance are similar to the case at 15.6 eV shown in Figure 5 where the laser excitation leads to a dissociation into the subunits, dimers and trimer, proceeding along the symmetry plane, although more gently in the present case.

4.3.4 Off resonant — high emission

Figure 8 shows results again for the case far below resonance but with larger intensity. The case resides in the regime of strong emission, as in Figure 6 (see Sect. 4.3.2). The pattern are much similar to Figure 6. The strong laser pulse removes the majority of the electrons. And again, a Coulomb explosion of the cluster follows immediately. It is interesting to note that the explosion path is much similar to the resonant case in Section 4.3.2. The dimer ions fly away quickly along the z-axis such that the expansion goes through strongly prolate shapes and the electron cloud decouples from the global ionic motion. This hints that the dynamical evolution becomes rather independent of the excitation frequency when considering the regime of strong emission. We have found that as a general feature in some other calculations with different excitation frequencies. On the other hand, the results hint that the explosion path strongly depends on the initial cluster geometry.

5 Conclusion

In this paper we have discussed the dynamical response of the H_9^+ cluster to a short and intense laser pulse. For this study we have used the TDLDA-MD approach which has proven to be a robust model for non-linear dynamics in simple metal clusters. The case of hydrogen clusters is a priori a bit more involved than simple metals due to a mix of bonding types. For example, H_9^+ is composed of three neutral dimers and one charged trimer which as such are strongly bound and tied together to the whole cluster by a weaker bonding. We have shown that the H_9^+ cluster with this loosely bound "molecular" structure can be perfectly well described with TDLDA, at least in its ground state for which our results compare well with other approaches. This alone is already an interesting outcome for what concerns the capability of DFT methods in such systems.

The main concern of this paper was an analysis of the dynamical response of this cluster to irradiation. We first briefly discussed the "optical" response as an observable

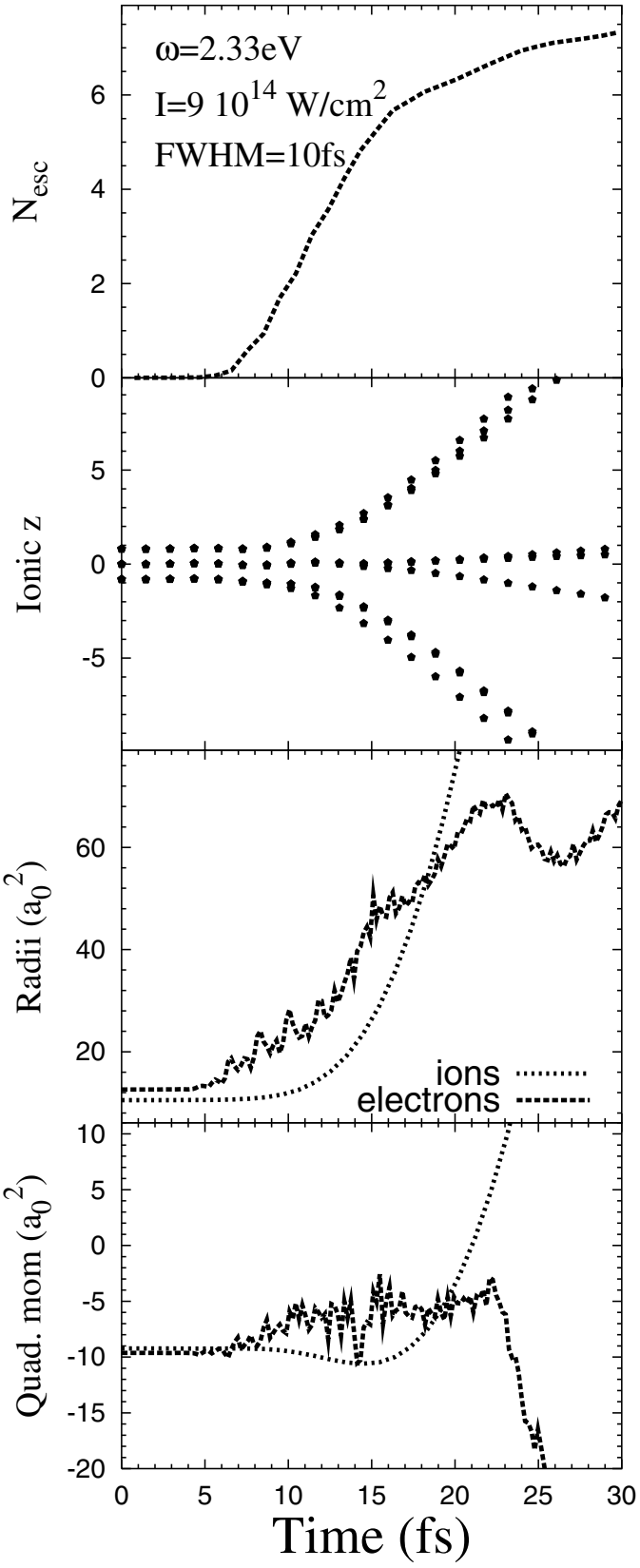

Fig. 8. As Figure 5, but for excitation far below resonance and large intensity.

in the "linear" domain which serves as a guideline for understanding the behavior of the system under stronger irradiations. We have then focused on various possible scenarios for the response to an intense laser pulse. We have shown that depending on the relation of the laser frequency to the eigenfrequencies of the system (in particular to the optical frequencies of both the dimers and trimer) one may observe various deexcitation/explosion scenarios. It so constitutes a nice example of coherent control, the switching of reaction paths by proper choice of laser parameters. These scenarios involve both electrons and ions but the relative role of each species does depend on the actual excitation conditions. The interference of electronic and ionic motion is particularly impressive in this case of hydrogen clusters in which the ionic and electronic time scales come closer than in any other molecular system.

The authors thank the French-German exchange program PROCOPE number 99074 and Institut Universitaire de France for financial support during the realization of this work.

References

1. U. Kreibig, M. Vollmer, *Optical properties of metal clusters* (Springer Series in Materials Science, 1993), Vol. 25
2. Faisal, *Theory of Multiphoton Processes* (Plenum Press, New York, 1987)
3. J. Zweiback et al., Phys. Rev. Lett. **84**, 2634 (2000)
4. L. Köller, M. Schumacher, J. Köhn, S. Teuber, J. Tiggesbäumker, K.-H. Meiwes-Broer, Phys. Rev. Lett. **82**, 3783 (1999)
5. P.-G. Reinhard, E. Suraud, *Introduction to Cluster Dynamics* (Wiley, Berlin, 2003)
6. *NATO ASI Series B*, edited by E.K.U. Gross, R.M. Dreizler (Plenum Press, New York, 1995), Vol. 337
7. F. Calvayrac, P.-G. Reinhard, E. Suraud, C. Ullrich, Phys. Rep. **337**, 493 (2000)
8. E. Suraud, P.-G. Reinhard, Phys. Rev. Lett. **85**, 2296 (2000)
9. F. Calvayrac, P.-G. Reinhard, E. Suraud, J. Phys. B **31**, 5023 (1998)
10. L.B. DaSilva et al., Phys. Rev. Lett. **78**, 483 (1997)
11. I. Štich, D. Marx, M.Parrinello, K. Terakura, J. Chem. Phys. **107**, 22 (1997)
12. H. Chermette, H. Razafinjanahary, L. Carrion, J. Chem. Phys. **107**, 24 (1997)
13. E. W. Ignacio, S. Yamabe, Chem. Phys. Lett. **287**, 563 (1997)
14. M. Barbatti, G. Jalbert, M.A.C. Nascimento, J. Chem. Phys. **113**, 4230 (2000)
15. *NATO ASI Series* B, edited by E.K.U Gross, R. M. Dreizler (Plenum Press, New York, 1995), Vol. 337
16. J.P. Perdew, Y. Wang, Phys. Rev. B **45**, 13244 (1992)
17. V. Blum, G. Lauritsch, J.A. Maruhn, P.-G. Reinhard, J. Comp. Phys **100**, 364 (1992)
18. M.D. Feit, J.A. Fleck, A. Steiger, J. Comp. Phys. **47**, 412 (1982)
19. L. Verlet, Phys. Rev. **159**, 98 (1967)
20. C.A. Ullrich, J. Mol. Struct. (THEOCHEM) **501-502**, 315 (2000)
21. L.M. Ma, E. Suraud, P.-G. Reinhard, Eur. Phys. J. D **14**, 217 (2001)
22. K. Yabana, G.F. Bertsch, Phys. Rev. B **54**, 4484 (1996)
23. F. Calvayrac, P.-G. Reinhard, E. Suraud, Ann. Phys. (NY) **255**. 125 (1997)
24. J.P. Perdew, K. Burke, M. Ernzerhof, Phys. Rev. Lett. **77**, 3865 (1996)
25. J.P. Perdew, A. Zunger, Phys. Rev. B **23**, 5048 (1981)
26. P.-G. Reinhard, F. Calvayrac, C. Kohl, S. Kümmel, E. Suraud, C.A. Ullrich, M. Brack, Eur. Phys. J. D **9**, 111 (1999)
27. C.A. Ullrich, P.-G. Reinhard, E. Suraud, J. Phys. B **30**, 5043 (1997)
28. S.M. Sze, C.R. Crowell, G.P. Carey, E.E. LaBate, J. Appl. Phys. **37**, 2690 (1996)
29. P.-G. Reinhard, E. Suraud, Eur. Phys. J. D **3**, 175 (1998)
30. P.-G. Reinhard, E. Suraud, Appl. Phys. B **73**, 401 (2001)